Published in final edited form as:
Anal Chem. 2009 September 1; 81(17): 7436–7442. doi:10.1021/ac9012072.

Aptamer-based microfluidic device for enrichment, sorting, and detection of multiple cancer cells

Ye Xu[a,b], **Joseph A. Phillips**[a], **Jilin Yan**[a], **Qingge Li**[b], **Z. Hugh Fan**[c,d], and **Weihong Tan**[a]

Z. Hugh Fan: hfan@ufl.edu; Weihong Tan: tan@chem.ufl.edu

[a]Center for Research at the Bio/Nano Interface, Department of Chemistry and Department of Physiology and Functional Genomics, Shands Cancer Center, UF Genetics Institute, and McKnight Brain Institute, University of Florida, Gainesville, Florida 32611-7200, USA, Fax: 352-392-0346; Tel: 352-846-2410

[b]Molecular Diagnostics Laboratory, Department of Biomedical Sciences and The Key Laboratory of the Ministry of Education for Cell Biology and Tumor Cell Engineering, School of Life Sciences, Xiamen University, Xiamen, Fujian 361005, China

[c]Department of Mechanical and Aerospace Engineering, University of Florida, P. O. Box 116250, Gainesville, FL 32611, USA

[d]Department of Biomedical Engineering, University of Florida, P. O. Box 116131, Gainesville, FL 32611, USA

Abstract

The ability to diagnose cancer based on the detection of rare cancer cells in blood or other bodily fluids is a significant challenge. To address this challenge, we have developed a microfluidic device that can simultaneously sort, enrich, and then detect multiple types of cancer cells from a complex sample. The device, which is made from poly(dimethylsiloxane) (PDMS), implements cell-affinity chromatography based on the selective cell-capture of immobilized DNA-aptamers and yields a 135-fold enrichment of rare cells in a single run. This enrichment is achieved because the height of the channel is on the order of a cell diameter. The sorted cells grow at the comparable rate as cultured cells and are 96% pure based on flow cytometry determination. Thus, by using our aptamer based device, cell capture is achieved simply and inexpensively, with no sample pretreatment before cell analysis. Enrichment and detection of multiple rare cancer cells can be used to detect cancers at the early stages, diagnose metastatic relapse, stratify patients for therapeutic purposes, monitor response to drugs and therapies, track tumor progression, and gain a deeper understanding of the biology of circulating tumor cells (CTCs).

Keywords

aptamer; microfluidic; multiplexed; enrichment; sorting

Introduction

It is estimated that a tumor can shed 10^6 cells per day into the bloodstream.[1, 2] Assuming no clearance of these cells from the blood stream yields an upper bound of 200 tumor cells/mL of blood in an average adult male human having approximately 5L of blood. This concentration represents about 0.004% of all the white cells in the blood and detecting these

Correspondence to: Z. Hugh Fan, hfan@ufl.edu; Weihong Tan, tan@chem.ufl.edu.

cells represents a clear challenge. Consequently, there is an ever-increasing need for isolation or enrichment of phenotypically pure cell subpopulations from a heterogeneous mixture of cells. To accomplish this, fluorescent activated cell sorting (FACS) is the most common method for affinity-based isolation. Cell mixtures are fluorescently labeled using specific dyes or antibodies to surface antigens and then sorted, one-by-one, based on light scattering and fluorescent properties. However, conventional flow cytometers tend to be large and expensive, requiring specially trained personnel for sample tagging and instrument operation.[3] Magnetic-activated cell sorting (MACS) is also used to isolate cells by a single parameter using antibody-coated magnetic beads.[4] Recent improvements, including sorting [5–7] and multiple parameter sorting[4, 8], make magnetic sorting a favorable alternative to FACS. Nonetheless, a defect of both FACS and MACS is the requirement for pre-processing incubation with various forms of antibody tags. The number of parameters accessible to separation is thus limited to the availability of distinct tags, such as antibody, fluorophore, and magnetiphoretic mobility of beads.[9]

Because of their small physical dimensions, microfluidic systems have, in contrast, shown unique promise for establishing inexpensive, simple, and fast assays for many different biological applications.[10–15] In recent years, investigators have taken several approaches to enrich or separate cells within microfluidic devices. The design principles are based on cell size, fluorescent or magnetic tagging of cells, electrophoretic mobility, and surface adhesion.[16] Specifically, as long as ligands for particular cell-surface receptors are known, these molecules can be immobilized onto the surface of a channel to achieve cell capture from a flowing suspension.[9, 17, 18] This approach is particularly attractive because no pre-processing incubation of the cell suspension is required. Using this strategy, surface-immobilized ligands have been utilized to capture subpopulations of several different cell types [18, 19], e.g., lymphocyte subpopulations, breast cancer cells, lung cancer cells, and endothelial cells. However, only a few highly selective and high-affinity antibodies or ligands are known for those target cells, effectively limiting the scope of these microfluidic devices. To solve this problem, DNA-aptamers were introduced into microfluidic device systems.[20]

Aptamers have been the focus of much recent work in cancer related research and development especially in potential diagnosis and therapy[21–24]. Briefly, aptamers are selected by an *in vitro* process known as cell-SELEX, or Systematic Evolution of Ligands by EXponential enrichment[25], from a pool of DNA or RNA candidates. Aptamers bind with high specificity and sensitivity to a variety of molecular or cellular targets. A series of aptamers have been created in our lab that target live cancer cells, including lymphocytic and myeloid leukemia[26, 27], small-cell lung cancer[28] and liver cancer cells.[29] As noted above, one drawback of current microfluidic systems is that few highly selective and high-affinity antibodies or ligands are known for those target cells. By contrast, however, one key benefit of using aptamers derived from cell-SELEX is precisely that these aptamers can be created without knowing the explicit molecular signature information that differentiates cancer cells from healthy cells. Because we can use a healthy cell as a control, and then use the target cancer cell to subtract the DNA sequences which bind to its cell-surface markers from the DNA library. Therefore, cell-SELEX aptamers can be used for detection and enrichment before the corresponding antibody has even been developed for a specific cancer.

Microfluidic cell-affinity chromatography devices can be used to capture cells from any patient sample that contains occult tumor cells. However, such devices are currently used for the accurate detection and molecular profiling of circulating tumor cells (CTCs).[30, 31] It has been shown that the number of CTCs in a patient sample correlates with clinical outcome.[32–34] Furthermore, CTCs are heterogeneous, and there is mounting evidence that

subpopulations of CTCs can target specific distant sites during metastasis.[35–39] At this time, most commercial technologies use Ep-CAM antibodies to detect CTCs, but the amount of Ep-CAM on tumor cells varies widely and depends on the tumor type[40], and there is a general lack of specific and high-affinity probes for live cell capture. Therefore, because cell-SELEX can be performed on any target cell-line, it is conceivable that aptamers can be produced that are specific for each subpopulation of CTCs. Moreover, since any aptamer can easily be modified and immobilized within a device, a multiplexed cell-capture device based on aptamers would eventually be useful in generating the molecular profile of CTCs from patient samples, ultimately allowing their detection and purification. This result could, in turn, lead to a number of potential benefits: detecting cancer at the early stages, diagnosing metastatic relapse, stratifying patients for therapeutic purposes, monitoring response to drugs and therapies, tracking tumor progression, and gaining a deeper understanding of the biology of CTCs.

We have previously demonstrated aptamer-based microfluidic devices in which target cells were isolated from a mixture of control cells via the specific capture of an immobilized aptamer.[20] These devices were based on the notion that a cell-affinity chromatography device with dimensions on the order of a cell's diameter, 10–20 μm, would significantly enhance rare-cell enrichment. Here, we extend our design in two ways. First, we demonstrate the capability of our device to simultaneously enrich multiple, distinct target cells into independent fractions. Second, we perform cell sorting of these cell fractions. As a model system, we chose to use three different leukemia cell lines for which we have three aptamers that bind each cell type selectively. Although this system does not represent a true CTC sample, we used it to develop the method that can quantitatively analyze the efficiency of microfluidic cell-affinity chromatography devices and optimize the device design. We found that the sorted cells grow at rates comparable to those of cultured cells with 96% purity based on flow cytometry analysis. We also investigated the enrichment efficiency of the device and found that target cells at 0.33% original purity could be enriched by a factor of > 130 times.

Experimental Section

Cell Culture and Buffers

CCRF-CEM cells (CCL-119 T-cell, human acute lymphoblastic leukemia), Ramos cells (CRL-1596, B-cell, human Burkitt's lymphoma), and Toledo cells (CRL-2631, non-Hodgkin's B-cell lymphoma) were obtained from ATCC (American Type Culture Association). The cells were cultured in RPMI medium 1640 (ATCC) supplemented with 10% FBS (heat-inactivated; GIBCO) and 100 IU/mL penicillin-Streptomycin (Cellgro). Immediately before experiments, cells were rinsed with washing buffer [4.5 g/L glucose and 5 mM $MgCl_2$ in Dulbecco's PBS with calcium chloride and magnesium chloride (Sigma)] and diluted to 1,000,000 cell/mL. Following the manufacturer's instructions, the cells were labeled with Vybrant DiI or Vybrant DiO cell-labeling solutions (Invitrogen) for 5 min at 37°C, rinsed with washing buffer, and re-suspended at 10,000,000 cell/mL in binding buffer [washing buffer supplemented with yeast tRNA (0.1 mg/mL; Sigma), BSA (1 mg/mL; Fisher), and 10% FBS]. Labeled cells were stored on ice and further diluted before experiments.

Device Fabrication and Operation

PDMS devices were fabricated using a process similar to what is described in the literature.[41] The layout of the device was designed in AutoCAD and printed on a transparency using a high-resolution printer. The pattern on the transparency was transferred to a silicon wafer via photolithography. The silicon wafer was etched to a depth of 40 μm in

a deep reactive ion-etching machine. The resulting silicon wafer with the desired pattern served as a mold to fabricate a number of PDMS devices. Following the manufacturer's instructions, Sylgard 184 (Corning) reagents were prepared and thoroughly mixed. After being degassed to remove bubbles, the mixture was cast on top of the silicon mold. After being cured at room temperature, the PDMS layer was peeled off the silicon mold. Punching holes in the PDMS created inlet and outlet wells. There are total of 4 wells along a serpentine channel as shown in Figure 1a. The PDMS slice was reversibly attached to a clean 50×45 mm no.1 cover glass (Fisher) to form a device. Avidin and DNA solutions were introduced into specific regions of the device by applying a vacuum to the appropriate pairs of wells as discussed in the next section. The surface modification chemistry has been previously described[20]. After device surfaces were modified with aptamers, cell solutions were introduced into the device by connecting a Micro4 syringe pump (World Precision Instruments, Inc.) to the outlet of the device. In between experiments, PDMS devices were cleaned by sequential sonication in 20% bleach with 0.1 M NaCl and then 50:1 water:versaclean (Fisher) at 40°C, followed by rinsing in deionized H_2O and drying under N_2.

Cell Capture Assay

Four wells were created in the S-shaped channel: two wells at the ends of the channel (denoted W1 and W4) and one well at each bend (denoted W2 and W3). These four holes divided the S-channel into three regions (denoted R1, R2, and R3). Avidin was first adsorbed to the glass surface of all three regions of the device by physically blocking W2 and W3 and pumping 20 μL avidin at 1 mg/mL (Invitrogen) in phosphate buffered saline through W1. To physically block the wells, PDMS was first polymerized within 10 μL pipette tips, and these tips were then inserted into the wells. Avidin was incubated for 15 seconds, and excess protein was rinsed by pumping 60 μL binding buffer through the device. Immobilization of multiple biotinylated aptamers to specific regions of the device was accomplished in the following manner. To immobilize the Sgc8 aptamer in R1, W3 and W4 were first blocked. Then, 10 μL of 20 μM Sgc8 in binding buffer was added to W1. A vacuum was then applied to W2 to force the Sgc8 into the R1 of the S-channel. After a 15-second incubation, R1 was rinsed with 30 μL of binding buffer. In the same manner, the other two aptamers, TD05 and Sgd5, were immobilized in R2 and R3, respectively. After all aptamers were immobilized, W2 and W3 were blocked, and W4 was connected to the syringe pump to apply negative pressure. Cells were mixed together in different ratios and diluted to specific concentrations in binding buffer with 10% FBS. To avoid cell settling, cell solution was dripped onto W1 of the device with a pipette. Pulses of 7 μL cell solution were incubated for 35 seconds, and a total of 70 or 700 μL was passed through the device, at which point a final rinse with 63 μL binding buffer was performed before imaging. The flow rate during cellcapture was set to 300 nL/s, using a Micro4 syringe pump.

Cell release

To release the sorted cells from the microfluidic device, air was pumped into each region of the S-channel separately. For example, for cells sorted from R1, air was pumped into W1 (200nL/s), while W3 and W4 were blocked, and the cell solution was accumulated at W2 and collected as the sorted fraction.

Microscopy, Image Analysis, and Flow Cytometry

In order to determine the cell surface density of each cell type, CEM and Ramos cells were labeled with red and green fluorescent stains, respectively, while Toledo cells were left unstained. After the cell-capture assay, image sets corresponding to red fluorescence, green fluorescence, and transmission images were obtained at 7 positions along each region of the device. Images were imported into ImageJ (NIH), the threshold was set to highlight

fluorescent cells, and cell counts were obtained using the Analyze Particles function. Cell counts were further confirmed by comparing fluorescent images with transmission images to verify cell morphology. The unlabeled Toledo cells were counted manually after overlaying the red and green fluorescent images onto the transmission image. The number of total cells captured was calculated by multiplying the average cell-surface density in each region by the surface area of the region. The enrichment purity was calculated by dividing the total number of target cells captured by the total number of cells captured in each region. The devices were imaged using an Olympus FV500-IX81 confocal microscope. Flow cytometry was performed with a FACScan cytometer (BD Immunocytometry Systems). Briefly, 1,000,000 cells were sequentially incubated with biotinylated DNA at 250 nM for 15 min in binding buffer, followed by incubation with streptavidin-PE (Invitrogen) following the manufacturer's instructions, and 30,000 counts were measured in the flow cytometer.

DNA Synthesis

aptamers Sgc8, TD05, and Sgd5 have been selected for CEM, Ramos, and Toledo cells, respectively: Sgc8 5′ - ATC TAA CTG CTG CGC CGC CGG GAA AAT ACT GTA CGG TTA GAT TTT TTT TTT - 3′ – Biotin; TD05 5′ - AAC ACC GGG AGG ATA GTT CGG TGG CTG TTC AGG GTC TCC TCC CGG TGT TTT TTT TTT - 3′ – Biotin; Sgd5 5′ - ATA CCA GCT TAT TCA ATT ATC GTG GGT CAC AGC AGC GGT TGT GAG GAA GAA AGG CGG ATA ACA GAT AAT AAG ATA GTA AGT GCA ATC T - 3′ – Biotin.[26, 27, 42] All aptamers were synthesized using an ABI3400 DNA/RNA synthesizer (Applied Biosystems). DNA synthesis reagents were purchased from Glen Research (Sterling, VA). DNA purification was performed with a ProStar HPLC (Varian) using a C18 column (Econosil, 5U, 250 × 4.6 mm) from Alltech Associates. UV-Vis measurements were performed with a Cary Bio-300 UV spectrometer (Varian) to measure DNA concentration.

Results and discussion

Device Design and operating procedure

Some elements of the device were designed according to our previously results.[20] The 40 μm height of the channel was designed for increasing cell capture efficiency. The 4 mm width of the channel gave a large surface area to capture cells. The serpent shape allowed more surface area to be contained in a smaller device. Wells separated the channel into 3 regions, in which 3 different aptamers were immobilized. This design allowed the cell mixture to be profiled within the device. When a cell mixture is passed through the device, each region can capture and enrich different cells based on aptamer binding. After the cell-capture assay, the device was imaged by confocal microscopy for detection of captured cells. For cell release, an air bubble was pumped into a specific region of the device, and the captured cells are collected by the meniscus.

Multiplexed cell detection

Our goal here was to create an inexpensive, simple, and fast multiplexed cancer detection platform. To achieve this goal, the advantages of DNA-aptamers generated by *in vitro* cell-SELEX and microfluidic devices were combined. We chose a microfluidic based device since these devices are inexpensive, easy to manufacture, and require small reagent volumes. When compared to antibodies, aptamers are easy to modify, reproducible to synthesize, have long shelf-lives, and can be de-natured and re-natured without loss of activity. Previous work has shown that aptamers immobilized within a microfluidic channel can be used to purify target cells from a background of non-target cells.[20] Since we had already selected aptamers for several different leukemia cell lines, a scheme that incorporates these aptamers at different regions within a device would extend this platform for multiplexed detection. We used an S-channel design to achieve this compartmentalization of cell-capture zones

(Figure 1A). The S-channel is segregated into three cell-capture regions by creating wells at each bend as shown in Figure 1A. By blocking different combinations of wells, three different aptamers can be immobilized in the three different regions of the device. Since there is no physical limit to the number of regions that can be added to the device, this design can be viewed as a universal design for multiplexed detection.

As proof-in-principle of this design, three different leukemia cell lines and their corresponding aptamers were used to test the simultaneous cell-capture capability of this device. Each aptamer was immobilized in a specific region within the device, and a mixture of the three cell lines was then pumped through the device. The immobilization of biotinylated aptamers to avidin adsorbed on the glass surface of the device is depicted in Figure 1B. To aid in the microscopic analysis of these experiments, two of the cell types were stained with different fluorescent membrane stains, while the third was left untreated. By design, each cell type within the cell mixture was captured on its respective aptamer-coated region, as shown in Figure 1C-E. This batch sorting represents the simultaneous enrichment and detection of three different types of cancer cells from a heterogeneous mixture of cancer cells. Because the aptamers used in these experiments show little or no binding to the non-target cell lines, the non-target cells are considered equivalent to healthy cells and, thus, as negative controls for each region. A final purity of over 97% was obtained for CEM and Ramos cells, and 88% for Toledo cells. Since these aptamers all have low nM dissociation constants, the lower percentage for Toledo cells may have been caused by a slight nonspecific binding of the Sgd5 aptamer to Ramos cells (data not shown), a steric affect from immobilization, or it may be that the protein target does not have an expression as high as the protein targets of Sgc8 and TD05 aptamers.[26, 27] Although the device has not been optimized for cell-capture efficiency, CEM, Ramos, and Toledo cells were captured at an efficiency of 83±9%, 61±14%, and 50±10%, respectively. The capture efficiencies and purities are similar to those reported in the literature for microfluidic cell-affinity chromatography devices, which ranged from 65% to 97% capture efficiency with 50% to 100% purity. [20, 31, 43]

Cell release and culture

After multiplexed detection by cell-capture, assays can be done within the device, such as cell proliferation,[44] counting,[19] and gene analysis.[45] On the other hand, since many more assays can be performed outside of the device, we were interested in investigating the feasibility of using this device to perform cell sorting. For effective cell sorting, two criteria must be met. First, the sorted cells must remain viable after the sorting process is finished. Second, sorted cells must be pure. One simple and gentle method to remove captured cells is to pump air through the device and allow the meniscus to strip the cells from the surface.[46] As Figure 2 shows, after air was pumped through the channel, most of the cells were released from the surface. In our hands, the collection efficiency was about 45%, since some cells were lost near the sides of the channel and at the dead volume in the wells. Out of focus spots where found to be residual liquid droplets attached to the PDMS surface (Figure S1). To test the viability of the sorted cells, we cultured them for several days afterwards. The growth curves shown in Figure 3 proved that the sorted cells were still viable. Furthermore, the slopes of the sorted cell growth curves were similar to the slopes of growth curves from cells that were never removed from culture, indicating that the capture and release process did not cause detectable cell death (Figure 3). The discrepancy in the initial growth rates for the sorted Toledo cells in comparison to the cultured Toledo cells in Figure 3c is due to the low initial concentration of the sorted cell sample. Although we cannot determine the exact cell concentration, it is much lower than the ideal cell culture concentrations ($3\times10^5 \sim 3\times10^6$ cells/mL) per the ATCC instructions. As a result, sorted Toledo cell has slightly slower growth rate than the culture. After growing for one day, the

slope of the sorted cell in figure 3c is comparable to that of the cultured cell data, indicated by parallel lines between 84- and 108-hour culturing. Next, the purity of the sorted cells was analyzed by flow cytometry. The sorted cells were grown for one week and then subjected to flow cytometry using all three aptamers and an unselected SELEX DNA-library as negative control. The data showed that the sorted and cultured cells had similar profiles by flow cytometric analysis (Figure S2). When compared to the aptamer binding profile of the cultured cells, the aptamer binding profile of the sorted cells revealed that the sorted cells were 96.5% pure.

Rare cell enrichment

After showing that our device could perform multiplexed detection and cell sorting, we wanted to establish the limit of this system to enrich rare populations of cells. The surface density and affinity of the aptamer, the microfluidic channel architecture , and the incubation time and flow rate of the cell solution during the experiment necessarily define the enrichment capability. Here, we chose R1 in the device to investigate the enrichment ability for rare cells in the cell mixture. The target cells (CEM) were labeled with red fluorescent membrane stain, and then mixtures of target and non-target cells were pumped through the device. Results of these experiments showed a parabolic dependence of cell surface purity relative to initial purity (Figure 4). A dependency of this nature can be modeled in a simple fashion by assuming that the number of captured cells is proportional to an efficiency multiplied by the initial cell concentrations:

$$\text{Cells captured} = E_t[\text{target}] + E_c[\text{control}], \tag{Eq.1}$$

where E_t and E_c are the target and control cell capture efficiencies, respectively. Because the total cell concentration was fixed in all of the enrichment experiments, we can parameterize the total cell concentration as [total] = [target] + [control] = P_t[total] + (1−P_t)[total]. Here, P_t is the percentage of target cells in the sample. Thus, equation (1) can be written:

$$\text{Cells captured} = \{P_t(E_t - E_c) + E_c\}[\text{total}]. \tag{Eq.2}$$

Using the definition of purity on the capture surface as the ratio of target cells captured to total cells captured, the purity can be written as:

$$\text{Purity} = P_t / \{P_t(1 - \varepsilon^{-1}) + \varepsilon^{-1}\}, \tag{Eq.3}$$

where ε is the capture efficiency ratio of the target to control efficiencies, E_t/E_c. The enrichment data from Figure 4 can be fit to this equation to yield the capture efficiency ratio, which, in this case, is ε^{-1} = 0.007 +/− 0.001. The capture efficiency ratio, ε, represents the maximum enrichment that is possible with this device operating under these specific conditions. Therefore, the theoretical limit of target cell capture efficiency is ε = 146 times the control cell capture efficiency. The capture efficiency ratio gives a good description of how well the device is operating. It is also an indicator of how the device can be used in future work to optimize new assemblies. The lowest initial concentration of 0.33% that we tested yielded a final enrichment of 45%, which represents 136-fold enrichment. Note that this capture efficiency reflects the layout of this device and the procedure used. Higher capture efficiency is expected from improved device design and protocol.

Conclusion

The ability to capture rare circulating tumor cells in microfluidic devices has gained attention recently.[30, 31] These microfluidic assays require no pretreatment of cells with molecular probes, and there is no physical limit to the number of cell surface markers that can be probed in these devices. We have shown the ability to perform multiplexed detection of cancer cells in such a microfluidic device, and we envision that simple devices like this can be designed in a way that allows clinicians to perform point-of-care molecular diagnosis and purification of live cells from bodily fluids of cancer patients. We have shown the ability to capture and sort cells without the use of lasers or any other sophisticated equipment. Furthermore, by employing our ability to sort cells, a sample can be passed sequentially through multiple sorting zones to arrive at a highly enriched sample. Although most groups have reported the ability to capture cells, none has reported a way to systematically compare one device or method to another. The enrichment factor, ε, as defined here, should give the community an independent measure of the enrichment capability of a given device and should also allow us to systematically investigate new device designs and assay parameters that can enhance the enrichment factor.

Future work will involve the selection of aptamers that target specific subtypes of CTCs and the development of prototype devices that incorporate the multiplexing and cell sorting capabilities into one integrated microfluidic system as well as developing automated systems for probe immobilization and sample injection. Furthermore, even though working with whole blood is the gold standard for point-of-care devices, many researchers save human blood samples after fractionation, in which case the buffy coat is the appropriate fraction to find rare cancer cells. In these types of samples, an immuno-depletion of healthy blood cells, e.g., using CD45,[47, 48] may yield an initial enrichment of ~100-fold. Therefore, a ~100,000-fold enrichment should be easily obtained when combined with microfluidic devices.

Supplementary Material

Refer to Web version on PubMed Central for supplementary material.

Acknowledgments

The authors would like to thank Ms. Yanrong Wu and Mr. Rahul R. Kamath for their helpful discussions and suggestions. This work is supported by NIH and NSF grants.

References

1. Liotta LA, Saidel MG, Kleinerman J. Cancer Res. 1976; 36:889–894. [PubMed: 1253177]
2. Butler TP, Gullino PM. Cancer Res. 1975; 35:512–516. [PubMed: 1090362]
3. Krüger J, Singh K, O'Neill A, Jackson C, Morrison A, O'Brien P. Journal of Micromechanics and Microengineering. 2002; 12:486–494.
4. Thiel A, Scheffold A, Radbruch A. Immunotechnology. 1998; 4:89–96. [PubMed: 9853950]
5. Haik Y, Pai V, Chen C. J Magnetism Magn Mater. 1999; 194:254–261.
6. McCloskey KE, Moore LR, Hoyos M, Rodriguez A, Chalmers JJ, Zborowski M. Biotechnol Prog. 2003; 19:899–907. [PubMed: 12790655]
7. Zborowski M, Sun L, Moore LR, Williams PS, Chalmers JJ. J Magnetism Magn Mater. 1999; 194:224–230.
8. Partington KM, Jenkinson EJ, Anderson G. J Immunol Methods. 1999; 223:195–205. [PubMed: 10089098]
9. Sin A, Murthy SK, Revzin A, Tompkins RG, Toner M. Biotechnol Bioeng. 2005; 91:816–826. [PubMed: 16037988]

10. Das C, Fredrickson CK, Xia Z, Fan ZH. Sens Actuators, A. 2007; 134:271–277.
11. Furdui VI, Harrison DJ. Lab Chip. 2004; 4:614–618. [PubMed: 15570374]
12. Liu RH, Yang J, Lenigk R, Bonanno J, Grodzinski P. Anal Chem. 2004; 76:1824–1831. [PubMed: 15053639]
13. Situma C, Hashimoto M, Soper SA. Biomol Eng. 2006; 23:213–231. [PubMed: 16905357]
14. Witek MA, Wei S, Vaidya B, Adams AA, Zhu L, Stryjewski W, McCarley RL, Soper SA. Lab Chip. 2004; 4:464–472. [PubMed: 15472730]
15. Yi C, Li C, Ji S, Yang M. Anal Chim Acta. 2006; 560:1–23.
16. Radisic M, Iyer RK, Murthy SK. Int J Nanomedicine. 2006; 1:3–14. [PubMed: 17722258]
17. Du Z, Colls N, Cheng KH, Vaughn MW, Gollahon L. Biosens Bioelectron. 2006; 21:1991–1995. [PubMed: 16242927]
18. Murthy SK, Sin A, Tompkins RG, Toner M. Langmuir. 2004; 20:11649–11655. [PubMed: 15595794]
19. Cheng X, Irimia D, Dixon M, Sekine K, Demirci U, Zamir L, Tompkins RG, Rodriguez W, Toner M. Lab Chip. 2007; 7:170–178. [PubMed: 17268618]
20. Phillips JA, Xu Y, Xia Z, Fan ZH, Tan W. Anal Chem. 2009; 81:1033–1039. [PubMed: 19115856]
21. Soundararajan S, Chen W, Spicer EK, Courtenay-Luck N, Fernandes DJ. Cancer Res. 2008; 68:2358–2365. [PubMed: 18381443]
22. Mi J, Zhang X, Rabbani ZN, Liu Y, Reddy SK, Su Z, Salahuddin FK, Viles K, Giangrande PH, Dewhirst MW, Sullenger BA, Kontos CD, Clary BM. Mol Ther. 2008; 16:66–73. [PubMed: 17912235]
23. Huang YF, Sefah K, Bamrungsap S, Chang HT, Tan W. Langmuir. 2008; 24:11860–11865. [PubMed: 18817428]
24. Smith JE, Medley CD, Tang Z, Shangguan D, Lofton C, Tan W. Anal Chem. 2007; 79:3075–3082. [PubMed: 17348633]
25. Stoltenburg R, Reinemann C, Strehlitz B. Biomol Eng. 2007; 24:381–403. [PubMed: 17627883]
26. Shangguan D, Li Y, Tang Z, Cao ZC, Chen HW, Mallikaratchy P, Sefah K, Yang CJ, Tan W. Proc Natl Acad Sci U S A. 2006; 103:11838–11843. [PubMed: 16873550]
27. Tang Z, Shangguan D, Wang K, Shi H, Sefah K, Mallikratchy P, Chen HW, Li Y, Tan W. Anal Chem. 2007; 79:4900–4907. [PubMed: 17530817]
28. Chen HW, Medley CD, Sefah K, Shangguan D, Tang Z, Meng L, Smith JE, Tan W. ChemMedChem. 2008; 3:991–1001. [PubMed: 18338423]
29. Shangguan D, Meng L, Cao ZC, Xiao Z, Fang X, Li Y, Cardona D, Witek RP, Liu C, Tan W. Anal Chem. 2008; 80:721–728. [PubMed: 18177018]
30. Maheswaran S, Sequist LV, Nagrath S, Ulkus L, Brannigan B, Collura CV, Inserra E, Diederichs S, Iafrate AJ, Bell DW. N Engl J Medicine. 2008; 359:366.
31. Nagrath S, Sequist LV, Maheswaran S, Bell DW, Irimia D, Ulkus L, Smith MR, Kwak EL, Digumarthy S, Muzikansky A, Ryan P, Balis UJ, Tompkins RG, Haber DA, Toner M. Nature. 2007; 450:1235–1239. [PubMed: 18097410]
32. Pantel K, Riethdorf S. Nat Rev Clin Oncol. 2009; 6:190–191. [PubMed: 19333222]
33. Pierga JY, Bidard FC, Mathiot C, Brain E, Delaloge S, Giachetti S, de Cremoux P, Salmon R, Vincent-Salomon A, Marty M. Clin Cancer Res. 2008; 14:7004–7010. [PubMed: 18980996]
34. Cristofanilli M, Budd GT, Ellis MJ, Stopeck A, Matera J, Miller MC, Reuben JM, Doyle GV, Allard WJ, Terstappen LW, Hayes DF. N Engl J Med. 2004; 351:781–791. [PubMed: 15317891]
35. Nguyen DX, Bos PD, Massague J. Nat Rev Cancer. 2009; 9:274–284. [PubMed: 19308067]
36. Attard G, Swennenhuis JF, Olmos D, Reid AH, Vickers E, A'Hern R, Levink R, Coumans F, Moreira J, Riisnaes R, Oommen NB, Hawche G, Jameson C, Thompson E, Sipkema R, Carden CP, Parker C, Dearnaley D, Kaye SB, Cooper CS, Molina A, Cox ME, Terstappen LW, de Bono JS. Cancer Res. 2009; 69:2912–2918. [PubMed: 19339269]
37. Chiang AC, Massague J. N Engl J Med. 2008; 359:2814–2823. [PubMed: 19109576]
38. Nguyen DX, Massague J. Nat Rev Genet. 2007; 8:341–352. [PubMed: 17440531]
39. Gupta GP, Massague J. Cell. 2006; 127:679–695. [PubMed: 17110329]

40. Pantel K, Brakenhoff RH, Brandt B. Nat Rev Cancer. 2008; 8:329–340. [PubMed: 18404148]
41. Duffy DC, McDonald JC, Schueller OJA, Whitesides GM. Anal Chem. 1998; 70:4974–4984. [PubMed: 21644679]
42. Shangguan D, Cao ZC, Li Y, Tan W. Clin Chem. 2007; 53:1153–1155. [PubMed: 17463173]
43. Adams AA, Okagbare PI, Feng J, Hupert ML, Patterson D, Gottert J, McCarley RL, Nikitopoulos D, Murphy MC, Soper SA. J Am Chem Soc. 2008; 130:8633–8641. [PubMed: 18557614]
44. Gu W, Zhu X, Futai N, Cho BS, Takayama S. Proc Natl Acad Sci U S A. 2004; 101:15861–15866. [PubMed: 15514025]
45. Marcus JS, Anderson WF, Quake SR. Anal Chem. 2006; 78:3084–3089. [PubMed: 16642997]
46. Barkley S, Johnson H, Eisenthal R, Hubble J. Biotechnol Appl Biochem. 2004; 40:145–149. [PubMed: 14670084]
47. Lara O, Tong X, Zborowski M, Chalmers JJ. Exp Hematol. 2004; 32:891–904. [PubMed: 15504544]
48. Bilkenroth U, Taubert H, Riemann D, Rebmann U, Heynemann H, Meye A. Int J Cancer. 2001; 92:577–582. [PubMed: 11304694]

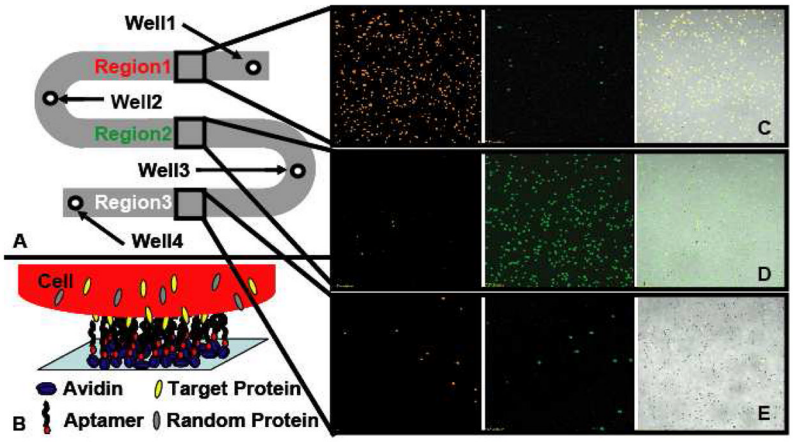

Figure 1. Microfluidic device and multiplexed detection of 3 different cancer cell lines

A) Schematic of microfluidic device, showing three regions used for aptamer immobilization and four wells used for channel preparation and cell sample injection. B) Representation of aptamer immobilization scheme, showing avidin adsorbed to the glass surface and biotinylated aptamers capturing a cell through specific molecular interactions. C–E) Representative image sets at one location within each aptamer coated region, showing red fluorescent images, green fluorescent images, and double overlays of the fluorescent channels with the transmission image. C) The sgc8 aptamer immobilized in Region1 specifically enriches the red -stained CEM cells. D) The TD05 aptamer immobilized in Region2 specifically enriches the green -stained Ramos cells. E) The Sgd5 aptamer immobilized in Region3 specifically enriches the unstained Toledo cells.

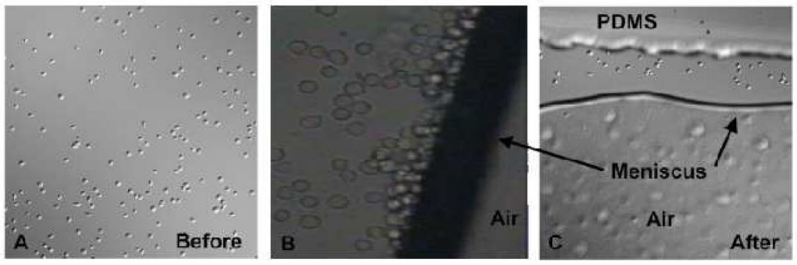

Figure 2. Cell release using an air bubble

A) DIC (Differential Interference Contrast) image of cells attached to aptamer -coated microchannel after cell capture assay. B) Phase contrast image of the moving meniscus at the front of the air bubble, with cells accumulating at the meniscus. C) DIC image of device after the air bubble has passed and the cells have been recovered. Some cells are left behind in the channel near the PDMS walls.

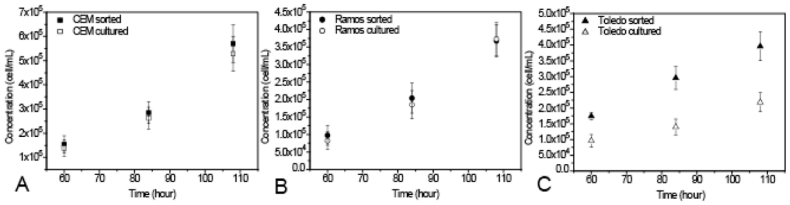

Figure 3. viability of sorted cells compared with cultured cells

Growth curves created by plotting cell concentration versus time show that sorted cells (filled symbols) grow at a similar rate compared to pure cells (open symbols). A, B, and C represent CEM, Ramos, and Toledo cell growth, respectively.

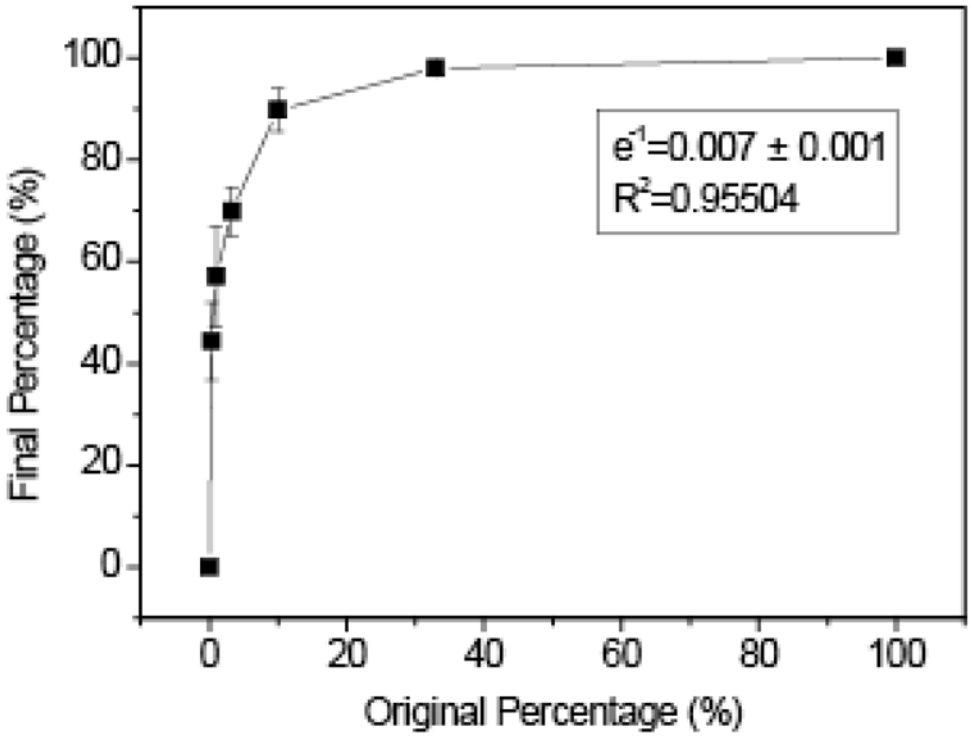

Figure 4. Final cell purity as a function of its initial concentration

CEM cells were spiked at various concentrations, and a final purity was plotted as a function of the initial cell concentration. The data were fit to equation 3, as indicated by the solid line. The ratio of control cell capture efficiency to target cell capture efficiency was 146.